Mechanism and Machine Theory 57 (2012) 95–110

Contents lists available at SciVerse ScienceDirect

Mechanism and Machine Theory

journal homepage: www.elsevier.com/locate/mechmt

Multiple linkage forms and bifurcation behaviours of the double-subtractive-Goldberg 6*R* linkage

C.Y. Song, Y. Chen *

School of Mechanical and Aerospace Engineering, Nanyang Technological University, Singapore, 50 Nanyang Avenue, 639798, Singapore

A R T I C L E I N F O

Article history:
Received 22 February 2012
Received in revised form 11 July 2012
Accepted 11 July 2012
Available online 17 August 2012

Keywords:
Subtractive Goldberg 5*R* linkage
Double-Goldberg 6*R* linkage
Bennett-based linkage
Bricard linkage

A B S T R A C T

In this paper, a particular type of double-subtractive-Goldberg 6*R* linkage is obtained by combining two subtractive Goldberg 5*R* linkages on the commonly shared 'roof-links' through the common link-pair method and common Bennett-linkage method. Two distinct linkage forms are obtained with the identical geometry conditions, yet different closure equations. Bifurcation behaviours of these two forms are analysed, leading to the discovery of two more linkage forms of this linkage, which cannot be constructed with Bennett linkages or Goldberg linkages directly. From the construction process, this 6*R* linkage belongs to the Bennett-based linkages. But about the bifurcation behaviours, it is closely related to the line-symmetric Bricard linkage because of its hidden symmetric property. Therefore, it could play an important role in exploring the relationship between the Bennett-based linkages and the Bricard linkages.

Notations

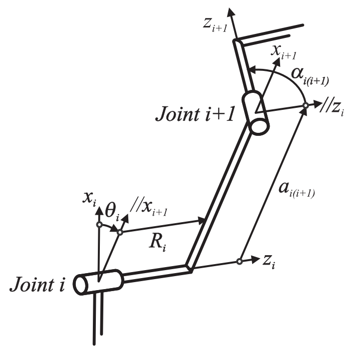

Spatial setup of the Denavit–Hartenberg's parameters.

* Corresponding author. Tel.: +65 6790 5941; fax: +65 6790 4062.
E-mail address: chenyan@ntu.edu.sg (Y. Chen).

0094-114X/$ – see front matter © 2012 Elsevier Ltd. All rights reserved.
http://dx.doi.org/10.1016/j.mechmachtheory.2012.07.002

z_i coordinate axis along the revolute axis of joint i;
x_i coordinate axis along the common normal from z_i to z_{i+1};
$a_{i(i+1)}$ length of link $i(i+1)$, which is the common normal distance from z_i to z_{i+1} positively about x_{i+1};
$\alpha_{i(i+1)}$ twist of link $i(i+1)$, which is the rotation angle from z_i to z_{i+1} positively about x_{i+1};
R_i offset of joint i, which is the common normal distance from x_i to x_{i+1} positively along z_i;
θ_i revolute variable of joint i, which is the rotation angle from x_i to x_{i+1} positively about z_i;
a/α, b/β, c/γ, d/δ the length and twist of the link, e.g. a/α is a link with length a and twist α;
$m_{1,2,\ldots,5}$, $P_{\mathrm{I,II}}$, Q, $A_{1,2,3,4}$, $B_{1,2,3,4}$, $S_{11,12,21,22}$ symbols for the simplified mathematical relationships;
A1, A2, A3, A4, B1, B2, B3, B4 different configurations of the 5R linkages A and B;
Forms I, II, III and IV different linkage forms of the double-subtractive-Goldberg 6R linkages;
$B_{\mathrm{I,II}}$, $B'_{\mathrm{I,II}}$ bifurcation points on the kinematic paths.

1. Introduction

The overconstrained linkage is a kind of mechanism that preserves mobility during a full-circle movement while not complying with the Grübler–Kutzbach's mobility criterion. There are a number of spatial overconstrained linkages with only revolute joints. Among them, the most famous one is the Bennett linkage [1,2], an overconstrained four-bar linkage with skew angle of twists. With proper arrangement and construction method, certain number of Bennett linkages can be combined together to build different types of single-loop overconstrained 5R and 6R linkages, called the Bennett-based linkages [3], including Goldberg's 5R and 6R linkages [4], Myard's 5R and 6R linkages [5], extended Myard linkage [6], one of the special Waldron's hybrid 6R linkages [7], Yu and Baker's syncopated 6R linkage [8], Wohlhart's double-Goldberg 6R linkage [9], back-to-back double-Goldberg 6R linkage [10], subtractive Goldberg 5R linkage , a special double-subtractive-Goldberg 6R linkage [11] and a family of mixed double-Goldberg 6R linkages [12]. All of them have one degree of freedom generally.

Another important 3D overconstrained linkage is the Bricard linkage [13,14], consisting of six distinct cases: the line-symmetric octahedral case, the plane-symmetric octahedral case, the doubly collapsible octahedral case, the line-symmetric case, the plane-symmetric case and the trihedral case. Baker [15] pointed out that the line-symmetric octahedral case is just a special case of the general line-symmetric case. Wohlhart [16] proposed a linkage with a shared transversal and partial symmetry. Recent works of Fowler and Guest [17,18] shows that symmetry does increase the mobility of the mechanism. The line or plane symmetry makes the Bricard linkages mobile. Any additional symmetric property can increase the mobility of the linkage infinitely or finitely. For example, Chen, You and Tarnai [19] proposed a three-fold-symmetric Bricard linkage with a bifurcation point when six links are collinear. Chen and Chai [20] studied a special type of Bricard linkage with both line and plane symmetry. In the investigation of its bifurcation behaviour, a complicated bifurcation loop among the line and plane symmetric Bricard linkage, plane symmetric Bricard linkage and spherical 4R linkage has been formed. Chai and Chen [21] found two closure forms, the linkage form and the structure form, in a special line-symmetric octahedral Bricard linkage.

Meanwhile, new reconfigurable mechanism has been proposed with multiple functions. The kinematotropic linkage by Wohlhart [22] can switch its global mobility at transit points. Dai and Rees [23] proposed the metamorphic mechanisms with variable topology and mobility. Kong and Huang [24] proposed a number of one degree-of-freedom overconstrained linkages with two operation modes by using the type synthesis method. Wohlhart [25] proposed a series of multifunctional 7R linkages by inserting an overconstrained mobile chain into a 7R linkage.

In this paper, a particular type of double-subtractive-Goldberg 6R linkage is introduced and multiple linkage forms are found, which shows great potential in application of reconfigurable mechanisms. The paper is presented as follows. Section 2 introduces the subtractive Goldberg 5R linkage. In Section 3, two linkage forms of the double-subtractive-Goldberg 6R linkage are built through different construction methods. Section 4 analyses their bifurcation behaviour, leading to two more linkage forms. Conclusion and discussions are drawn in Section 5.

2. The subtractive goldberg 5R linkage

As shown in Fig. 1, two Bennett linkages share a common link marked in grey. Using Goldberg's method [4], these two linkages are then inversely posed and superposed on the common link. After removing the common parts in dash lines, a subtractive Goldberg 5R linkage is constructed [11].

The geometry conditions of the linkage are

$$\begin{aligned}
&a_{12}=a_{34},\ a_{23}=a_{45}-a_{51},\\
&\alpha_{12}=\alpha_{34},\ \alpha_{23}=\alpha_{45}-\alpha_{51},\\
&\frac{\sin\alpha_{45}}{a_{45}}=\frac{\sin\alpha_{51}}{a_{51}}=\frac{\sin\alpha_{12}}{a_{12}},\\
&R_i=0(i=1,\ 2,\ldots,\ 5).
\end{aligned} \tag{1}$$

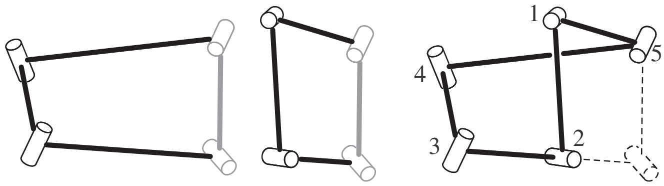

Fig. 1. Construction of the subtractive Goldberg 5*R* linkage.

Its closure equations are

$$\tan\frac{\theta_2}{2}=\frac{\tan\frac{\theta_1}{2}\sin\frac{\alpha_{12}+\alpha_{51}}{2}}{\sin\frac{\alpha_{12}-\alpha_{51}}{2}}, \tag{2a}$$

$$\tan\frac{\theta_3}{2}=\frac{\sin\frac{\alpha_{12}+\alpha_{45}}{2}}{\tan\frac{\theta_1}{2}\sin\frac{\alpha_{12}-\alpha_{45}}{2}}, \tag{2b}$$

$$\theta_4=-\theta_1, \tag{2c}$$

$$\tan\frac{\theta_5}{2}=\frac{\tan^2\frac{\theta_1}{2}+\frac{\sin\frac{\alpha_{12}+\alpha_{45}}{2}}{\sin\frac{\alpha_{12}-\alpha_{45}}{2}}\cdot\frac{\sin\frac{\alpha_{12}+\alpha_{51}}{2}}{\sin\frac{\alpha_{12}-\alpha_{51}}{2}}}{\left(\frac{\sin\frac{\alpha_{12}+\alpha_{45}}{2}}{\sin\frac{\alpha_{12}-\alpha_{45}}{2}}-\frac{\sin\frac{\alpha_{12}+\alpha_{51}}{2}}{\sin\frac{\alpha_{12}-\alpha_{51}}{2}}\right)\tan\frac{\theta_1}{2}}. \tag{2d}$$

Rewriting Eq. (2d) gives

$$\tan^2\frac{\theta_1}{2}-\left(\frac{\sin\frac{\alpha_{12}+\alpha_{45}}{2}}{\sin\frac{\alpha_{12}-\alpha_{45}}{2}}-\frac{\sin\frac{\alpha_{12}+\alpha_{51}}{2}}{\sin\frac{\alpha_{12}-\alpha_{51}}{2}}\right)\tan\frac{\theta_5}{2}\tan\frac{\theta_1}{2}+\frac{\sin\frac{\alpha_{12}+\alpha_{45}}{2}}{\sin\frac{\alpha_{12}-\alpha_{45}}{2}}\cdot\frac{\sin\frac{\alpha_{12}+\alpha_{51}}{2}}{\sin\frac{\alpha_{12}-\alpha_{51}}{2}}=0. \tag{2e}$$

So θ_1 in term of θ_5 can be presented as

$$\begin{aligned}\tan\frac{\theta_1}{2}=&\frac{1}{2}\left(\frac{\sin\frac{\alpha_{12}+\alpha_{45}}{2}}{\sin\frac{\alpha_{12}-\alpha_{45}}{2}}-\frac{\sin\frac{\alpha_{12}+\alpha_{51}}{2}}{\sin\frac{\alpha_{12}-\alpha_{51}}{2}}\right)\tan\frac{\theta_5}{2}\\&\pm\frac{1}{2}\sqrt{\left(\frac{\sin\frac{\alpha_{12}+\alpha_{45}}{2}}{\sin\frac{\alpha_{12}-\alpha_{45}}{2}}-\frac{\sin\frac{\alpha_{12}+\alpha_{51}}{2}}{\sin\frac{\alpha_{12}-\alpha_{51}}{2}}\right)^2\tan^2\frac{\theta_5}{2}-4\frac{\sin\frac{\alpha_{12}+\alpha_{45}}{2}}{\sin\frac{\alpha_{12}-\alpha_{45}}{2}}\cdot\frac{\sin\frac{\alpha_{12}+\alpha_{51}}{2}}{\sin\frac{\alpha_{12}-\alpha_{51}}{2}}}.\end{aligned} \tag{2f}$$

From Eq. (2f), it is obvious that there are two θ_1s corresponding to one θ_5, whereas θ_1 is one-to-one related to $\theta_{2,3,4}$, as shown in Eqs. (2a)–(2c). This property leads to a special characteristic of the double-subtractive-Goldberg 6*R* linkage constructed by two such 5*R* linkages, which shall be investigated next.

3. The double-subtractive-Goldberg 6*R* linkage

Two construction methods have been used in generating the complete set of mixed double-Goldberg 6*R* linkages [12]. The common link-pair (CLP) method, which was firstly proposed by Wohlhart [9] when building his double-Goldberg 6*R* linkage, is to achieve a single-loop overconstrained 6*R* linkage by merging two 5*R* linkages on the commonly shared link-pairs and then removing this connection. And the common Bennett-linkage (CBL) method, which was proposed by Song and Chen [11], is to connect the commonly shared link-pairs consecutively to build a common Bennett linkage as the connection. After removing the connection, the rest part will also form a single-loop overconstrained 6*R* linkage.

In order to get the double-subtractive-Goldberg 6*R* linkage by connecting two subtractive Goldberg 5*R* linkages on the "roof-links" through two construction methods, both subtractive Goldberg 5*R* linkages, namely linkages A and B, are required to share the same geometry conditions on link-pair 45–51 set as a/α~c/γ. Thus, the two sets of geometry conditions of linkages A and B are

$$
\begin{aligned}
&a_{12}^{A}=a_{34}^{A}=b,\ a_{23}^{A}=a-c,\ a_{45}^{A}=a,\ a_{51}^{A}=c,\\
&\alpha_{12}^{A}=\alpha_{34}^{A}=\beta,\ \alpha_{23}^{A}=\alpha-\gamma,\ \alpha_{45}^{A}=\alpha,\ \alpha_{51}^{A}=\gamma;\\
&a_{12}^{B}=a_{34}^{B}=d,\ a_{23}^{B}=a-c,\ a_{45}^{B}=a,\ a_{51}^{B}=c,\\
&\alpha_{12}^{B}=\alpha_{34}^{B}=\delta,\ \alpha_{23}^{B}=\alpha-\gamma,\ \alpha_{45}^{B}=\alpha\alpha_{51}^{B}=\gamma;\\
&\text{and } \frac{\sin\alpha}{a}=\frac{\sin\beta}{b}=\frac{\sin\gamma}{c}=\frac{\sin\delta}{d},\\
&R_i^{A}=R_i^{B}=0(i=1,\ 2,\ldots,\ 5).
\end{aligned}
\tag{3}
$$

Meanwhile, under the CLP method, these two subtractive Goldberg 5*R* linkages must have the same configuration on link-pair 45–51, i.e. $\theta_5^A=\theta_5^B$. And under the CBL method, the configurations of link-pair 45–51 in both linkages must meet the requirement of the Bennett linkage, i.e. $\theta_5^A+\theta_5^B=0$ or $\theta_5^A+\theta_5^B=2\pi$. In another words, for the linkage B with configuration $\theta_5^B=\psi$, only the

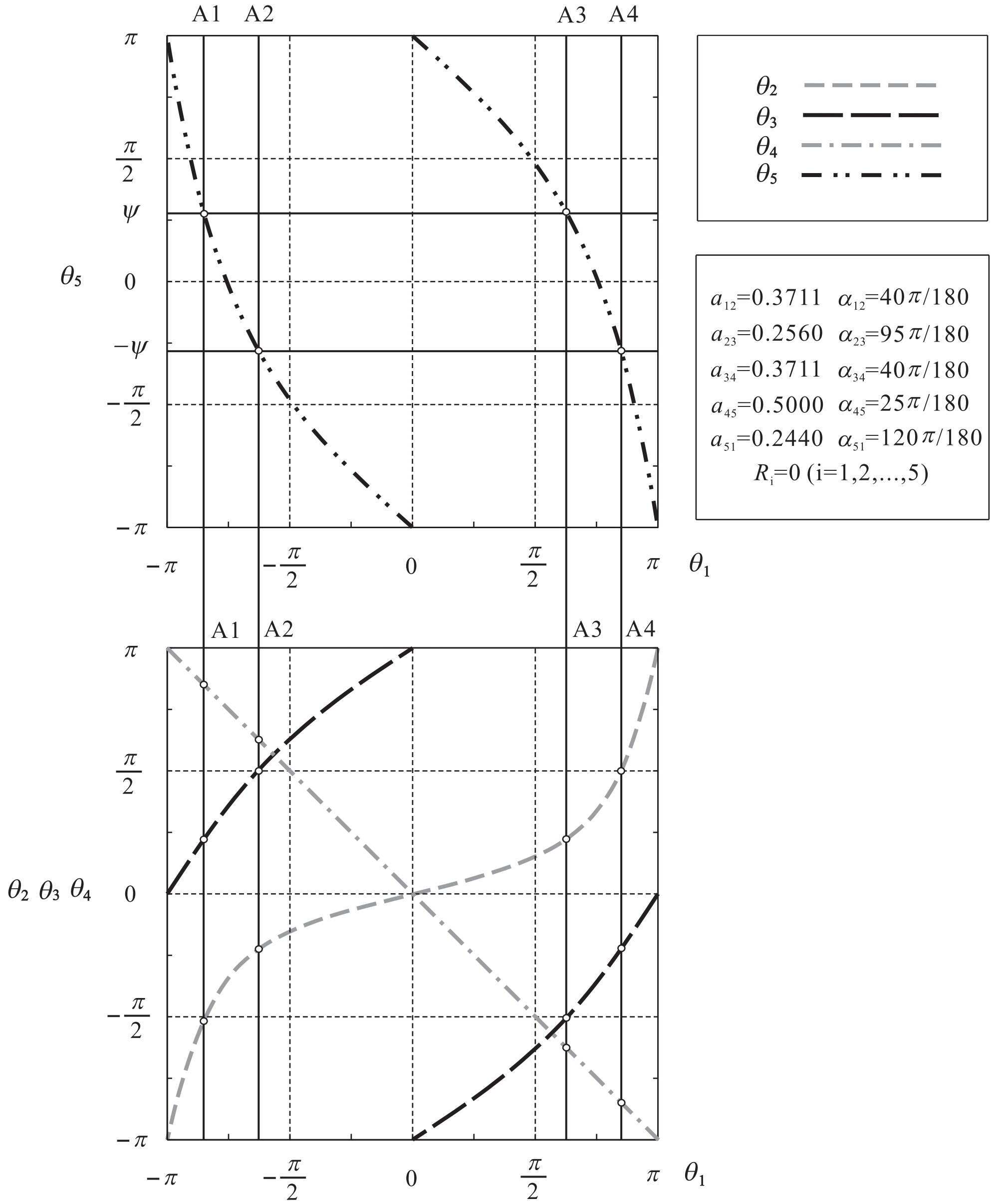

Fig. 2. The kinematic paths of linkage A, configurations A1 and A3 when $\theta_5^A=\psi$ and configurations A2 and A4 when $\theta_5^A=-\psi$.

linkage A with configuration $\theta_5^{A}=\psi$ can be used to form a 6*R* linkage through CLP method. And for the same linkage B, only the linkage A with configuration $\theta_5^{A}=-\psi$ can be used to form a 6*R* linkage through CBL method.

Due to the quadratic property between θ_1^{A} and θ_5^{A} on the kinematic path of linkage A in Fig. 2, there are two configurations of linkage A, A1 and A3, when $\theta_5^{A}=\psi$. Similarly, there are another two configurations of linkage A, A2 and A4, when $\theta_5^{A}=-\psi$. These four configurations are shown in Fig. 3, in which link-pair 45–51 is marked in grey colour, with $\theta_5^{A1}=\theta_5^{A3}=\psi$, and $\theta_5^{A2}=\theta_5^{A4}=-\psi$. Considering Eq. (2f), we have

$$\tan\frac{\theta_1^{A1,A3}}{2}=\frac{1}{2}\left(\frac{\sin\frac{\beta+\alpha}{2}}{\sin\frac{\beta-\alpha}{2}}-\frac{\sin\frac{\beta+\gamma}{2}}{\sin\frac{\beta-\gamma}{2}}\right)\tan\frac{\psi}{2}\pm\frac{1}{2}\sqrt{\left(\frac{\sin\frac{\beta+\alpha}{2}}{\sin\frac{\beta-\alpha}{2}}-\frac{\sin\frac{\beta+\gamma}{2}}{\sin\frac{\beta-\gamma}{2}}\right)^2\tan^2\frac{\psi}{2}-4\frac{\sin\frac{\beta+\alpha}{2}}{\sin\frac{\beta-\alpha}{2}}\cdot\frac{\sin\frac{\beta+\gamma}{2}}{\sin\frac{\beta-\gamma}{2}}},\tag{4a}$$

and

$$\tan\frac{\theta_1^{A2,A4}}{2}=-\frac{1}{2}\left(\frac{\sin\frac{\beta+\alpha}{2}}{\sin\frac{\beta-\alpha}{2}}-\frac{\sin\frac{\beta+\gamma}{2}}{\sin\frac{\beta-\gamma}{2}}\right)\tan\frac{\psi}{2}\mp\frac{1}{2}\sqrt{\left(\frac{\sin\frac{\beta+\alpha}{2}}{\sin\frac{\beta-\alpha}{2}}-\frac{\sin\frac{\beta+\gamma}{2}}{\sin\frac{\beta-\gamma}{2}}\right)^2\tan^2\frac{\psi}{2}-4\frac{\sin\frac{\beta+\alpha}{2}}{\sin\frac{\beta-\alpha}{2}}\cdot\frac{\sin\frac{\beta+\gamma}{2}}{\sin\frac{\beta-\gamma}{2}}}.\tag{4b}$$

Thus $\theta_1^{A1}=-\theta_1^{A4}$ and $\theta_1^{A2}=-\theta_1^{A3}$. And from the closure equations of the 5*R* linkage in Eqs. (2a)–(2d) and Eqs. (4a) and (4b), it is shown that $\theta_i^{A1}=-\theta_i^{A4}$ and $\theta_i^{A2}=-\theta_i^{A3}$ $(i=1,\ 2,\ldots,\ 5)$. Therefore, linkages A1 and A4 are in the same configuration, but their axes are in opposite directions. So are linkages A2 and A3.

As a result, the linkage B with configuration $\theta_5^{B}=\psi$ can be combined with linkages A1 and A3 through CLP method, and it can be combined with linkages A2 and A4 through CBL method. Similarly, for linkage B there are also two configurations, namely B1 and B3, when $\theta_5^{B}=\psi$ and another two configurations, namely B2 and B4, when $\theta_5^{B}=-\psi$, given in Fig. 4.

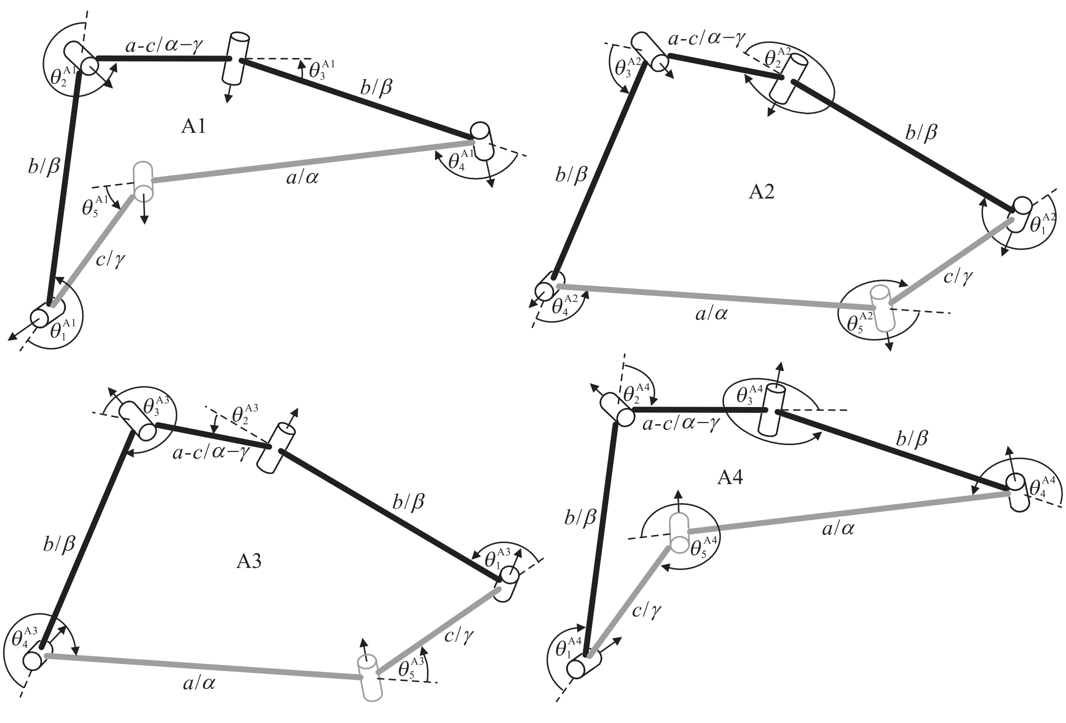

Fig. 3. The spatial configurations of A1, A2, A3 and A4, in which A1 and A3 are at $\theta_5^{A}=\psi$ and A2 and A4 are at $\theta_5^{A}=-\psi$.

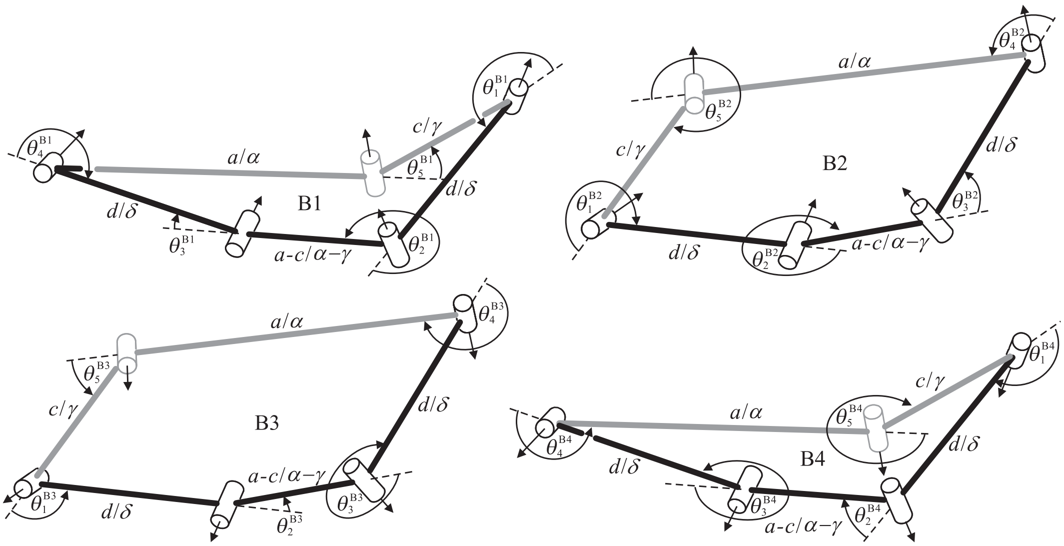

Fig. 4. The spatial configurations of B1, B2, B3 and B4, in which B1 and B3 are at $\theta_5^{\mathrm{B}}=\psi$ and B2 and B4 are at $\theta_5^{\mathrm{B}}=-\psi$.

Therefore, between one of the four linkage As and one of the four linkage Bs, only one construction method, CLP or CBL, can be applied to form a 6*R* linkage. Altogether, there will be 16 $(=4\times4)$ possible connections, among which only two distinct forms, Forms I and II linkages, are obtained as listed in Table 1. The third row will be taken as an example to explain the construction process in the following sections.

3.1. The Form I of the double-subtractive-Goldberg 6R linkage

Through the CLP method, linkages A1 and B3 are merged on the commonly shared link-pair 45–51 to form a single-loop overconstrained 6*R* linkage, named as Form I linkage, see Fig. 5. From Eq. (3), the geometry conditions of the 6*R* linkage are

$$\begin{aligned}
&a_{12}=a_{45}=a-c,\ a_{23}=a_{61}=d,\ a_{34}=a_{56}=b,\\
&\alpha_{12}=\alpha_{45}=\alpha-\gamma,\ \alpha_{23}=\alpha_{61}=\delta,\ \alpha_{34}=\alpha_{56}=\beta,\\
&\frac{\sin\alpha}{a}=\frac{\sin\beta}{b}=\frac{\sin\gamma}{c}=\frac{\sin\delta}{d},\\
&R_i=0(i=1,\ 2,\dots,6).
\end{aligned} \tag{5}$$

From the construction process, the closure equations of the Form I linkage can be derived as Eqs. (6a), (6b), (6c) and (6d). The kinematic paths of the linkage are plotted in Fig. 6.

$$\begin{aligned}
&\tan\frac{\theta_2}{2}=\frac{m_3}{m_4\tan\frac{\theta_1}{2}},\ \theta_3=\pi+2\tan^{-1}P_{\mathrm{I}}-2\tan^{-1}\left(m_4\tan\frac{\theta_1}{2}\right),\\
&\tan\frac{\theta_4}{2}=-\frac{m_1}{P_{\mathrm{I}}},\ \tan\frac{\theta_5}{2}=-\frac{P_{\mathrm{I}}}{m_2},\ \theta_6=\pi-2\tan^{-1}P_{\mathrm{I}}+2\tan^{-1}\left(m_4\tan\frac{\theta_1}{2}\right),
\end{aligned} \tag{6a}$$

Table 1
Sixteen possible connections between linkage As and linkage Bs.

	Linkage A1 $\theta_5^{\mathrm{A}}=\psi$	Linkage A2 $\theta_5^{\mathrm{A}}=-\psi$	Linkage A3 $\theta_5^{\mathrm{A}}=\psi$	Linkage A4 $\theta_5^{\mathrm{A}}=-\psi$
Linkage B1 $\theta_5^{\mathrm{B}}=\psi$	CLP-Form II	CBL-Form II	CLP-Form I	CBL-Form I
Linkage B2 $\theta_5^{\mathrm{B}}=-\psi$	CBL-Form II	CLP-Form II	CBL-Form I	CLP-Form I
Linkage B3 $\theta_5^{\mathrm{B}}=\psi$	CLP-Form I	CBL-Form I	CLP-Form II	CBL-Form II
Linkage B4 $\theta_5^{\mathrm{B}}=-\psi$	CBL-Form I	CLP-Form I	CBL-Form II	CLP-Form II

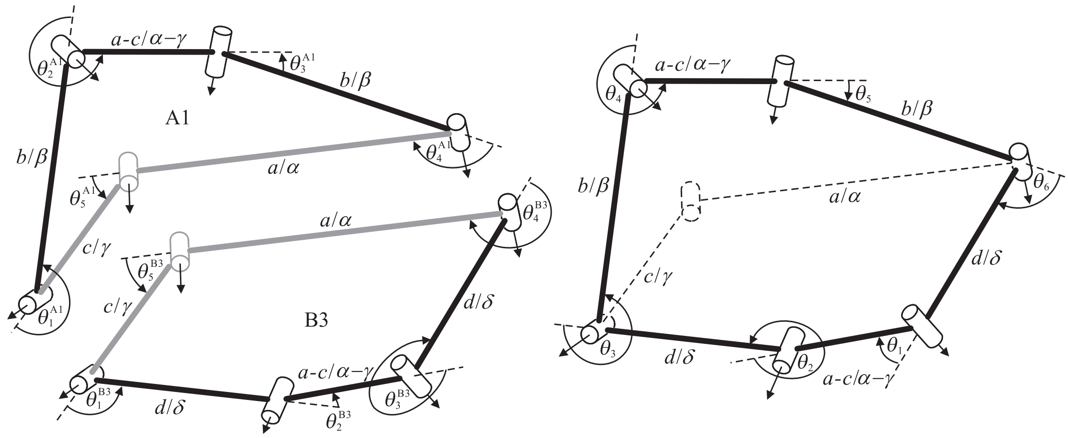

Fig. 5. The construction of the Form I linkage through CLP method.

where

$$P_1 = \begin{cases} \frac{1}{2}\left[(m_2 - m_1)Q + \sqrt{(m_2 - m_1)^2 Q^2 - 4m_1 m_2}\right] & \theta_1 \in [-\pi,\ 0) \\ \frac{1}{2}\left[(m_2 - m_1)Q - \sqrt{(m_2 - m_1)^2 Q^2 - 4m_1 m_2}\right] & \theta_1 \in [0,\ \pi) \end{cases}, \tag{6b}$$

$$Q = \frac{m_3 + m_4 \tan^2 \frac{\theta_1}{2}}{(m_4 - m_3)\tan \frac{\theta_1}{2}}. \tag{6c}$$

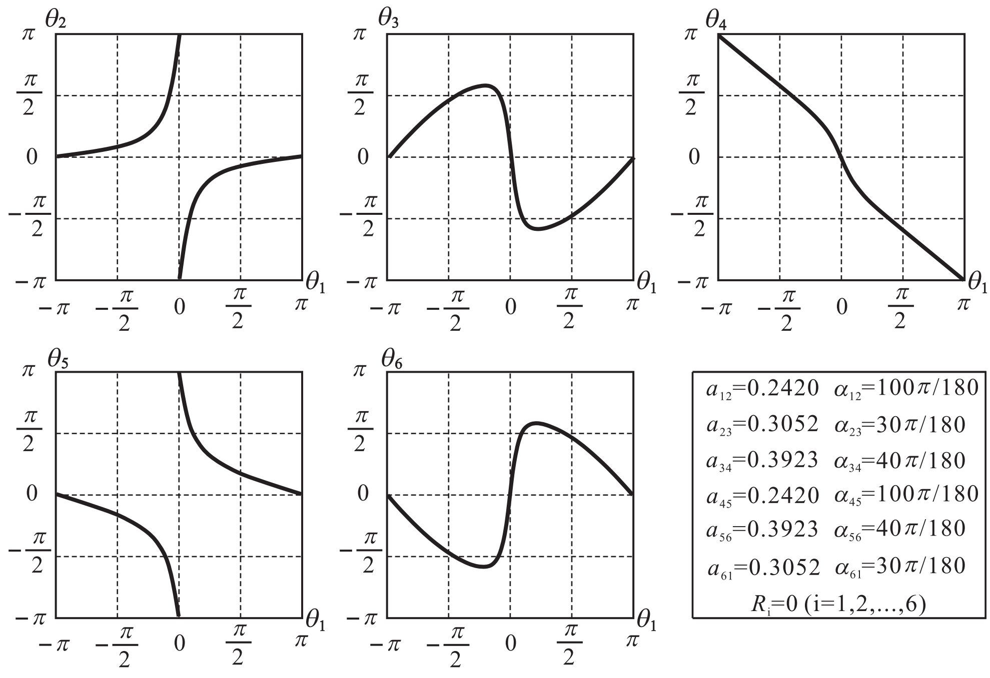

Fig. 6. The kinematic paths of the Form I linkage.

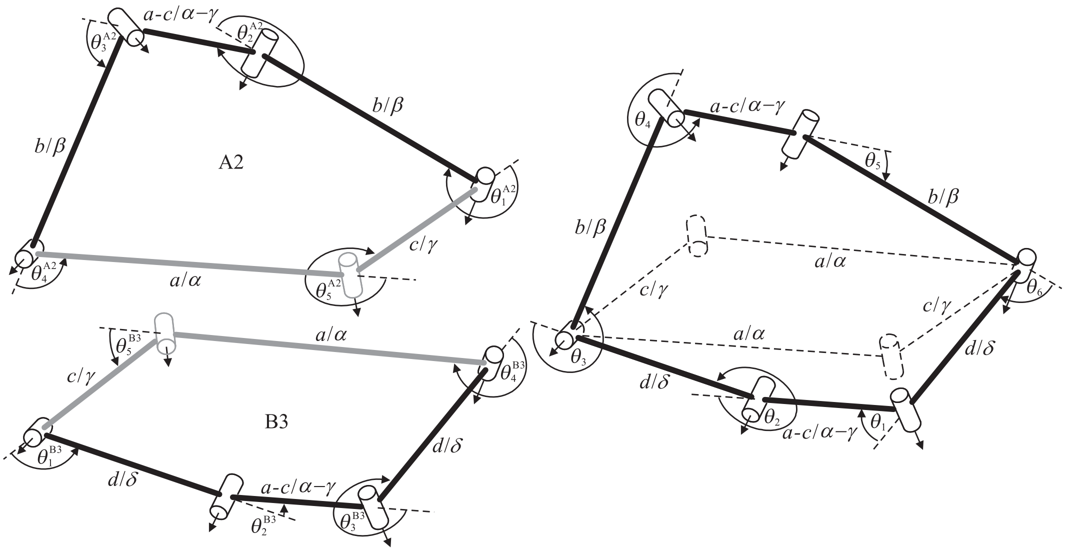

Fig. 7. The construction of the Form I linkage through CBL method.

and

$$m_1=\frac{\sin\frac{\beta+\alpha}{2}}{\sin\frac{\beta-\alpha}{2}},\ m_2=\frac{\sin\frac{\beta+\gamma}{2}}{\sin\frac{\beta-\gamma}{2}},\ m_3=\frac{\sin\frac{\delta+\alpha}{2}}{\sin\frac{\delta-\alpha}{2}},$$
$$m_4=\frac{\sin\frac{\delta+\gamma}{2}}{\sin\frac{\delta-\gamma}{2}},\ m_5=\frac{\sin\frac{\delta+\beta}{2}}{\sin\frac{\delta-\beta}{2}}. \tag{6d}$$

Alternatively, the same linkage can be obtained when linkages A2 and B3 are combined through CBL method, as shown in Fig. 7. Following a similar derivation process, the same closure equations as Eqs. (6a), (6b), (6c) and (6d) can be obtained.

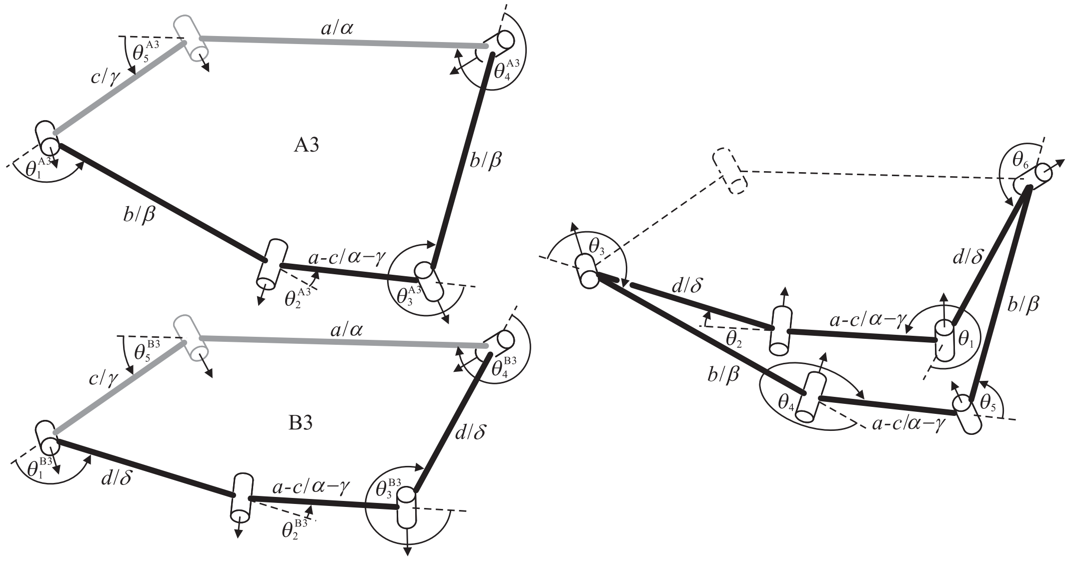

Fig. 8. The construction of the Form II linkage through CLP method.

3.2. The Form II of the double-subtractive-Goldberg 6R linkage

As shown in Fig. 8, linkages A3 and B3 are merged on link-pair 45–51 through CLP method to form a single-loop overconstrained 6*R* linkage. Obviously, the geometry conditions of this linkage are the same as those of the Form I linkage in Eq. (5). From the construction process, the closure equations of this linkage can be derived as Eq. (7) and the kinematic paths of the linkage are plotted in Fig. 9, which are different from those of the Form I linkage's. So we name this linkage as Form II linkage.

$$\begin{aligned}
&\tan\frac{\theta_2}{2}=\frac{m_3}{m_4\tan\frac{\theta_1}{2}},\ \theta_3=\pi+2\tan^{-1}P_{\mathrm{II}}-2\tan^{-1}\left(m_4\tan\frac{\theta_1}{2}\right),\\
&\tan\frac{\theta_4}{2}=-\frac{m_1}{P_{\mathrm{II}}},\ \tan\frac{\theta_5}{2}=-\frac{P_{\mathrm{II}}}{m_2},\ \theta_6=\pi-2\tan^{-1}P_{\mathrm{II}}+2\tan^{-1}\left(m_4\tan\frac{\theta_1}{2}\right),
\end{aligned}\tag{7}$$

where

$$P_{\mathrm{II}}=\begin{cases}\frac{1}{2}\left[(m_2-m_1)Q-\sqrt{(m_2-m_1)^2Q^2-4m_1m_2}\right] & \theta_1\in[-\pi,\ 0)\\ \frac{1}{2}\left[(m_2-m_1)Q+\sqrt{(m_2-m_1)^2Q^2-4m_1m_2}\right] & \theta_1\in[0,\ \pi)\end{cases},$$

and Q, and m_i are given in Eqs. (6c) and (6d).

Alternatively, the same linkage can be obtained with linkages A4 and B3 through CBL method, see Fig. 10. The same closure equations can be derived as Eq. (7).

After a throughout analysis of all sixteen possible constructions in Table 1, it is concluded that only Forms I and II linkages can be formed. They are the linkage forms with the identical geometry conditions but different kinematic paths. And there is no intersection between these two sets of kinematic paths, i.e., there is no common configuration. So they cannot transform into each other directly. These two linkage forms are in different and independent mobile closures.

4. Bifurcation analysis of the double-subtractive-Goldberg 6*R* linkage

It is worth noting that for both linkage forms, there exists such configuration on the kinematic paths, see Figs. 6 and 9, that all θ_i ($i=1, 2,\ldots, 6$) reach 0 or $\pm\pi$ simultaneously, which corresponds to the configuration that all six links are collinear. It is necessary to investigate such configurations for singularity. Recently, Müller [26,27] systematically investigated the generic mobility of rigid body mechanisms and its configuration space in regular and singular points. In this paper, the singular value decomposition (SVD) method of Jacobian matrix [28–30] is applied. The sixth singular value is always zero, which confirms that

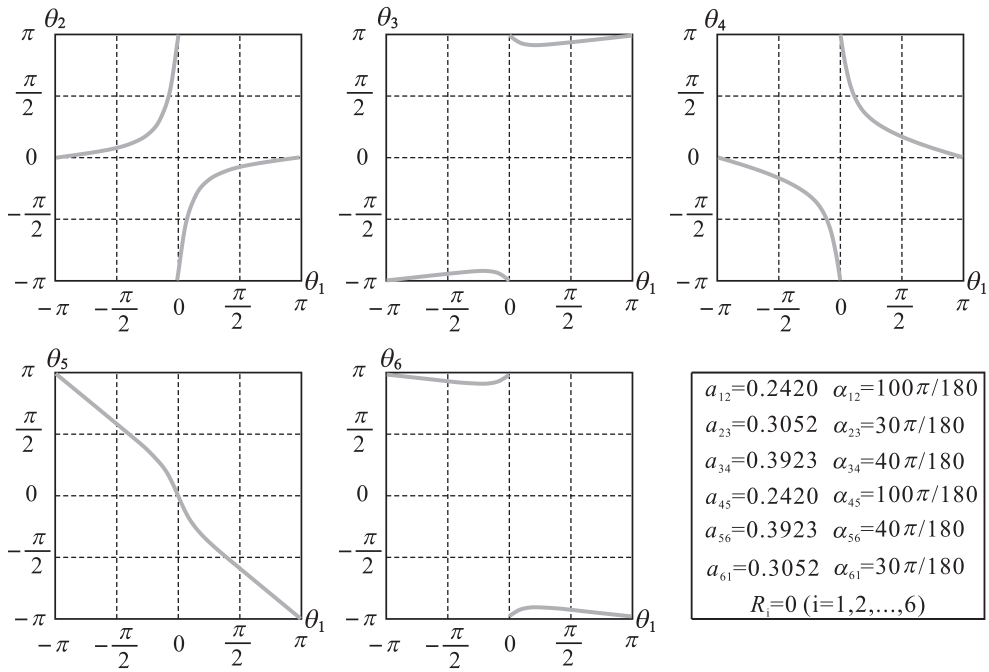

Fig. 9. The kinematic paths of the Form II linkage.

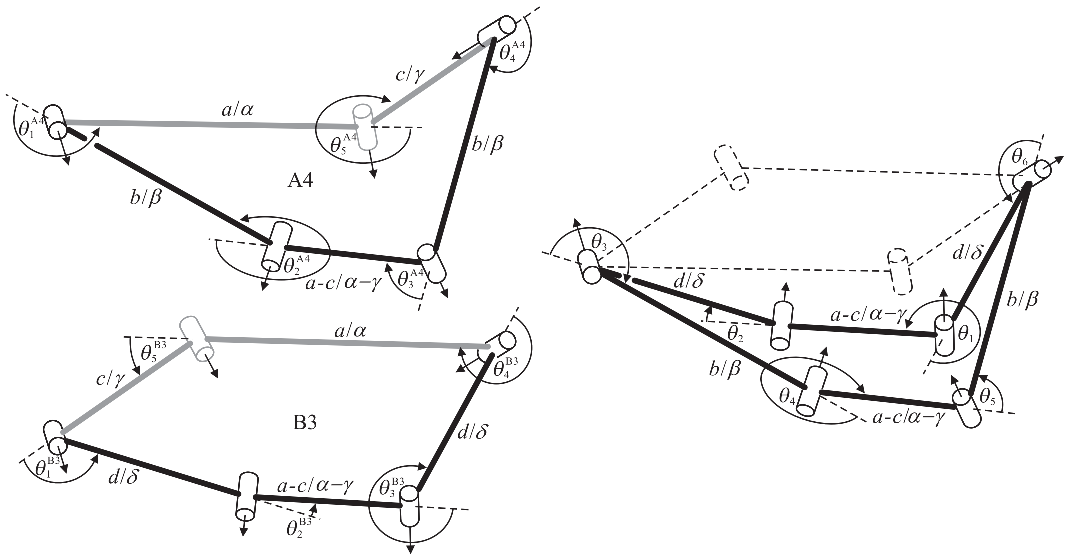

Fig. 10. The construction of the Form II linkage through CBL method.

the linkage has one degree of freedom during full-circle movement. At the collinear configurations, the fifth singular value falls to zero, which indicates that the instantaneous mobility is increased at these points.

The SVD results of the Forms I and II linkages are shown in Fig. 11. It is obvious that at the positions when $\theta_1=0$ and $\theta_1=\pm\pi$, the fifth singular value falls to zero. Thus, they are the bifurcation points. As there is no intersection between the kinematic paths of the Forms I and II linkages, it is expected that there are new possible kinematic paths between these bifurcation points.

4.1. The Form III of the double-subtractive-Goldberg 6R linkage

Through the SVD analysis, it is found that at the point $\theta_1^{\mathrm{I}}=0$ in Fig. 11(a), the Form I linkage can bifurcate into a different linkage form, namely the Form III linkage, as shown in Fig. 12. The Form II linkage can also bifurcate into the same linkage form at the point $\theta_1^{\mathrm{II}}=\pm\pi$ in Fig. 11(b).

The Form III linkage cannot be built from the combination of two subtractive Goldberg 5*R* linkages as Forms I and II linkages. By using the transformation matrix [31], the closure equations as Eqs. (9a) and (9b) are obtained analytically and the kinematic paths are shown in Fig. 13.

$$\begin{aligned}
&\theta_2=\pi+2\tan^{-1}S_{22}-2\tan^{-1}\frac{m_5}{S_{11}},\ \tan\frac{\theta_3}{2}=\ \tan\frac{\theta_6}{2}=S_{11},\\
&\theta_4=\pi+\theta_1+2\tan^{-1}\frac{m_5}{S_{11}},\ \tan\frac{\theta_5}{2}=S_{22}.
\end{aligned}\tag{8a}$$

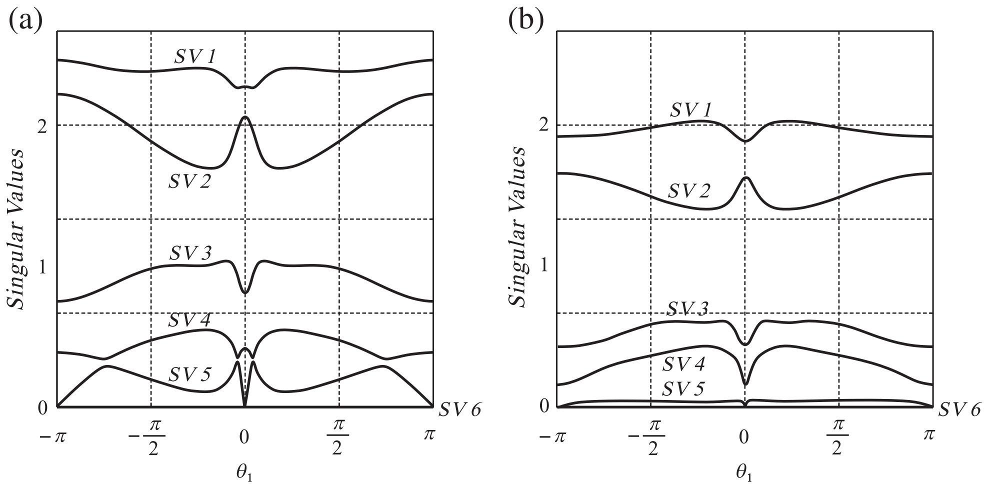

Fig. 11. The SVD results of (a) the Form I linkage and (b) the Form II linkage.

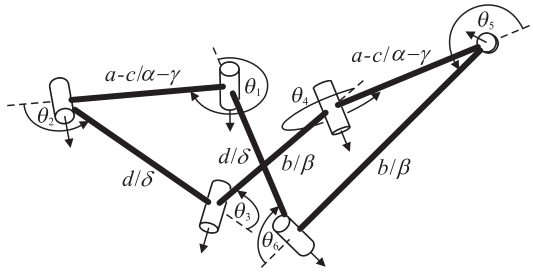

Fig. 12. The spatial layout of the Form III linkage.

where

$$\begin{cases} S_{11} = \dfrac{-(B_1 + D_1 \cos\theta_1) + \sqrt{(B_1 + D_1 \cos\theta_1)^2 - (A_1^2 - C_1^2)\sin^2\theta_1}}{(A_1 - C_1)\sin\theta_1} \\ S_{22} = \dfrac{-(B_2 + D_2 \cos\theta_1) - \sqrt{(B_2 + D_2 \cos\theta_1)^2 - (A_2^2 - C_2^2)\sin^2\theta_1}}{(A_2 - C_2)\sin\theta_1} \end{cases}, \tag{8b}$$

$$\begin{cases} A_1 = a_{34}\sin\alpha_{12} + a_{12}\sin\alpha_{34}\cos\alpha_{23} \\ B_1 = a_{34}\sin\alpha_{23} + a_{23}\sin\alpha_{34}\cos\alpha_{12} \\ C_1 = a_{23}\sin\alpha_{12} + a_{12}\sin\alpha_{23}\cos\alpha_{34} \\ D_1 = a_{12}\sin\alpha_{23} + a_{23}\sin\alpha_{12}\cos\alpha_{34} \end{cases}, \begin{cases} A_2 = a_{12}\sin\alpha_{34} + a_{34}\sin\alpha_{12}\cos\alpha_{23} \\ B_2 = a_{12}\sin\alpha_{23} + a_{23}\sin\alpha_{12}\cos\alpha_{34} \\ C_2 = a_{23}\sin\alpha_{34} + a_{34}\sin\alpha_{23}\cos\alpha_{12} \\ D_2 = a_{34}\sin\alpha_{23} + a_{23}\sin\alpha_{34}\cos\alpha_{12} \end{cases}, \tag{8c}$$

and m_5 is given in Eq. (6d).

The relationship between θ_1 and θ_5 of Forms I, II and III linkages is shown in Fig. 14. B_{I} is the bifurcation point between Forms I and III linkages, and B_{II} is the bifurcation point between Forms II and III linkages.

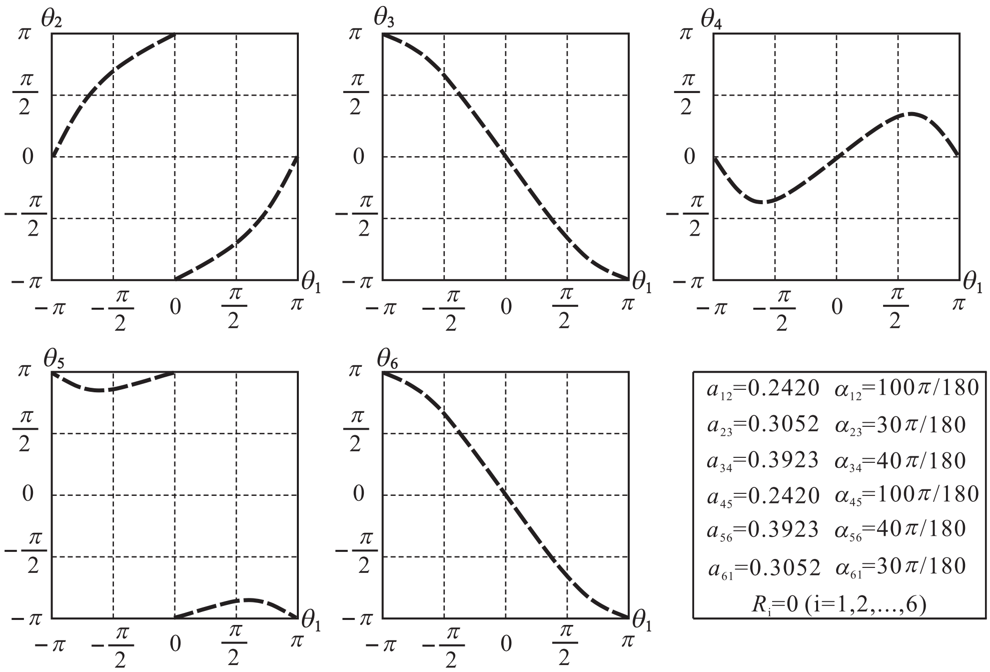

Fig. 13. The kinematic paths of the Form III linkage.

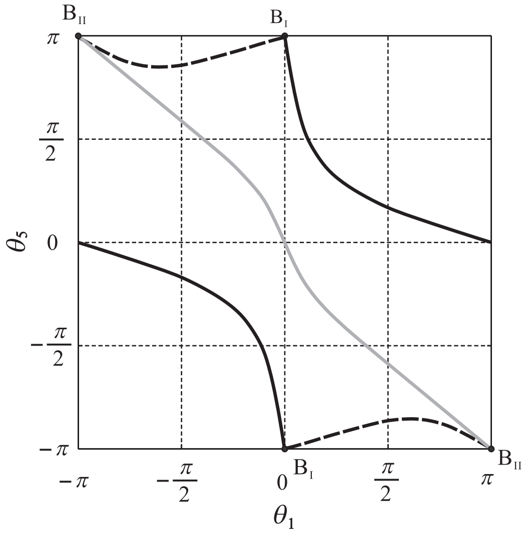

Fig. 14. The kinematic paths of Forms I, II and III linkages. The black solid lines are for Form I linkage, the grey solid lines are for Form II linkage and the black dash lines are for Form III linkage.

4.2. The Form IV of the double-subtractive-Goldberg 6R linkage

Furthermore, at the point $\theta_1^{\mathrm{I}}=\pm\pi$ in Fig. 11(a), the Form I linkage can bifurcate into another linkage form, namely the Form IV linkage, as shown in Fig. 15. The Form II linkage can also bifurcate into the Form IV linkage at the point $\theta_1^{\mathrm{II}}=0$ in Fig. 11(b).

Similar to the Form III linkage, the Form IV linkage also has no construction basis. By using the transformation matrix, the closure equations can be derived as Eqs. (9a) and (9b) and the kinematic paths are plotted in Fig. 16.

$$\begin{aligned}&\theta_2=\pi+2\tan^{-1}S_{21}-2\tan^{-1}\frac{m_5}{S_{12}},\ \tan\frac{\theta_3}{2}=\tan\frac{\theta_6}{2}=S_{12},\\&\theta_4=\pi+\theta_1+2\tan^{-1}\frac{m_5}{S_{12}},\ \tan\frac{\theta_5}{2}=S_{21},\end{aligned}\tag{9a}$$

where

$$\begin{cases}S_{12}=\dfrac{-(B_1+D_1\cos\theta_1)-\sqrt{(B_1+D_1\cos\theta_1)^2-\left(A_1^2-C_1^2\right)\sin^2\theta_1}}{(A_1-C_1)\sin\theta_1},\\[2ex] S_{21}=\dfrac{-(B_2+D_2\cos\theta_1)+\sqrt{(B_2+D_2\cos\theta_1)^2-\left(A_2^2-C_2^2\right)\sin^2\theta_1}}{(A_2-C_2)\sin\theta_1}.\end{cases}\tag{9b}$$

Note that A_i, B_i, C_i, D_i $(i=1,\ 2)$ and m_5 are given in Eqs. (8c) and (6d).

The relationship between θ_1 and θ_5 of Forms I, II and IV linkages is shown in Fig. 17. B'_{I} is the bifurcation point between Forms I and IV linkages, and B'_{II} is the bifurcation point between Forms II and IV linkages.

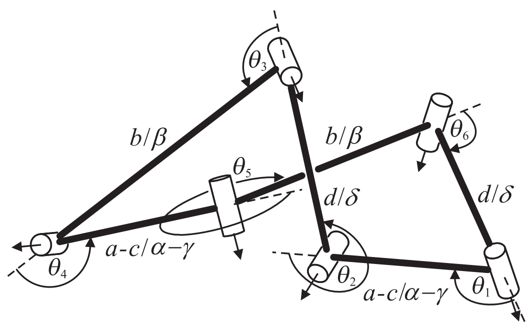

Fig. 15. The spatial layout of the Form IV linkage.

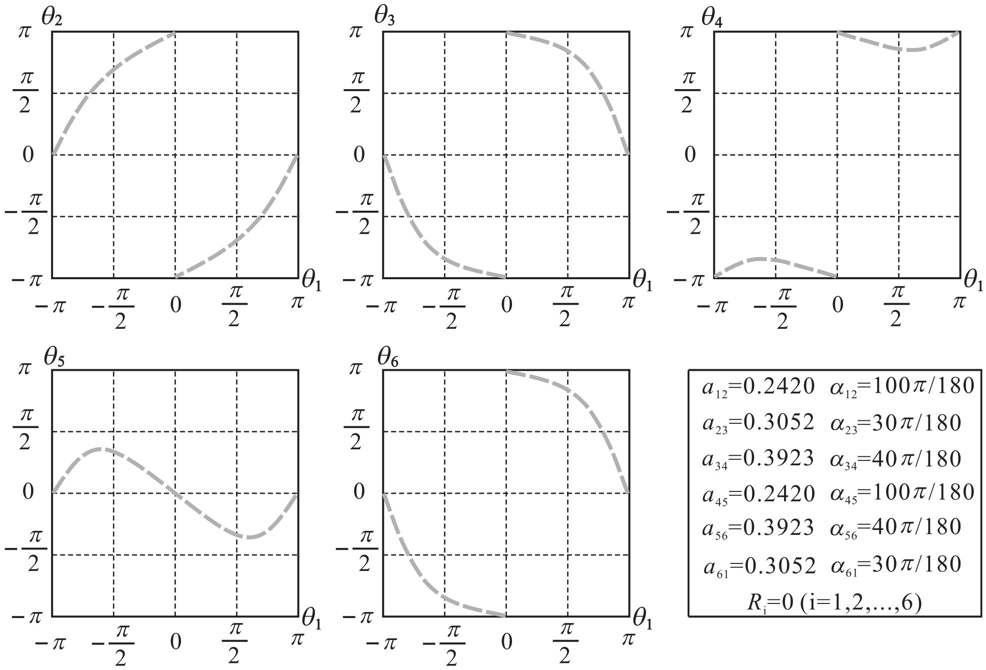

Fig. 16. The kinematic paths of the Form IV linkage.

Careful examination shows that the Forms III and IV linkages are actually the same linkage in different numbering sequences of joints. As shown in Fig. 18, after changing the numbering sequence in squares into that in circles, the representation of the geometry conditions of the linkage remains the same. In another words, the relationship between revolute variables of the Forms III and IV linkages are

$$\begin{aligned} &\theta_1^{\mathrm{III}} = \theta_2^{\mathrm{IV}}, \theta_2^{\mathrm{III}} = \theta_1^{\mathrm{IV}}, \theta_3^{\mathrm{III}} = \theta_6^{\mathrm{IV}}, \\ &\theta_4^{\mathrm{III}} = \theta_5^{\mathrm{IV}}, \theta_5^{\mathrm{III}} = \theta_4^{\mathrm{IV}}, \theta_6^{\mathrm{III}} = \theta_3^{\mathrm{IV}}. \end{aligned} \tag{10}$$

In summary, among the kinematic paths of all four forms of the double-subtractive-Goldberg 6*R* linkage, there are four different bifurcation points. The relationship between θ_1 and θ_5 is used to demonstrate the transformation among Forms I, II, III and IV linkages, as shown in Fig. 19.

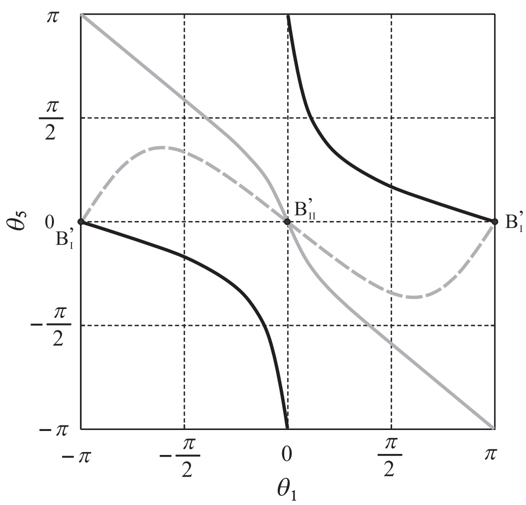

Fig. 17. The kinematic paths of Forms I, II and IV linkages. The black solid lines are for Form I linkage, the grey solid lines are for Form II linkage and the grey dash lines are for Form IV linkage.

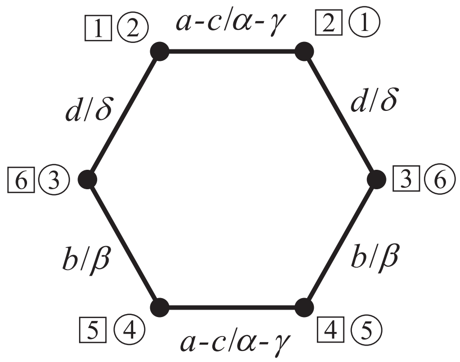

Fig. 18. The geometric conditions of the double-subtractive-Goldberg 6R linkage. The numbering sequence in squares correspond to the Form III linkage and the numbering sequence in circles correspond to the Form IV linkage.

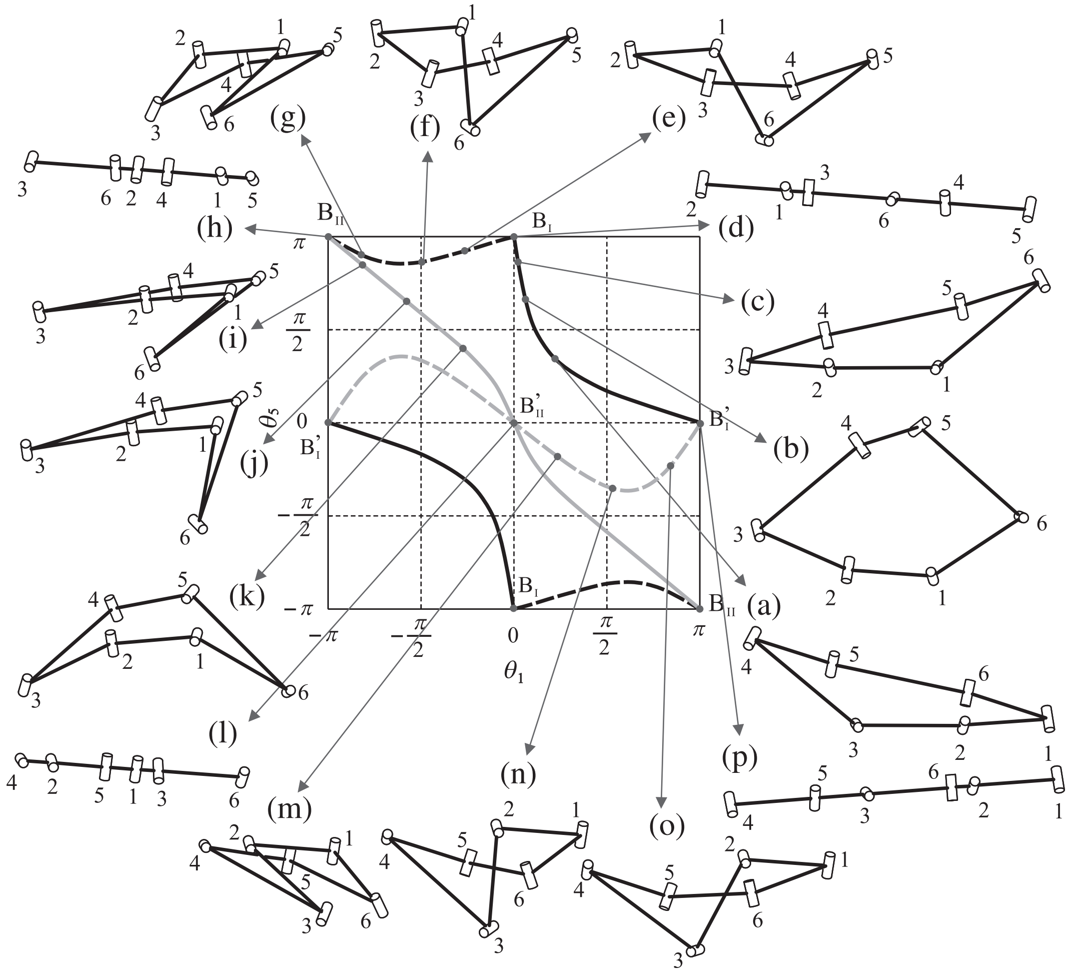

Fig. 19. Transformation among four forms of the double-subtractive-Goldberg linkage. The black and grey solid lines are for Form I and Form II linkages, and the black and grey dash lines are for Form III and Form IV linkages. (a)–(c) are the motion sequence of the Form I linkage; (d) is the bifurcation configuration B_I between Forms I and III linkages; (e)–(g) are the motion sequence of Form III linkage; (h) is the bifurcation configuration B_{II} between Forms III and II linkages; (i)–(k) are the motion sequence of the Form II linkage; (l) is the bifurcation configuration B'_{II} between Forms II and IV linkages; (m)–(o) are the motion sequence of Form IV linkage; and (p) is the bifurcation configuration B'_I between Forms I and IV linkages.

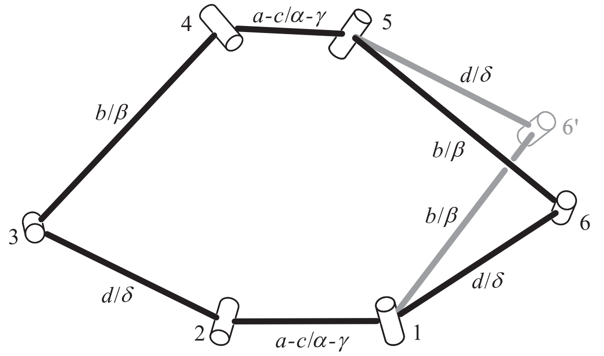

Fig. 20. Isomerization on the double-subtractive-Goldberg 6*R* linkage.

5. Conclusion and discussions

In this paper, due to the quadratic property of the revolute variable on the roof links of the subtractive Goldberg 5*R* linkage, two different and independent mobile closures of the double-subtractive-Goldberg 6*R* linkage, Forms I and II linkages, have been obtained by combining two subtractive Goldberg 5*R* linkages through common link-pair and common Bennett-linkage methods. Bifurcation analysis has been performed, leading to another two linkage forms, Forms III and IV linkages, which cannot be formed from the construction of Bennett-based linkages directly. Further investigation has revealed that the Forms III and IV linkages are actually the same linkage form in different numbering sequences. The kinematic paths of these four double-subtractive-Goldberg 6*R* linkage forms are connected through four bifurcation points to form a kinematic loop.

The bifurcation behaviour shown in this double-subtractive-Goldberg 6*R* linkage is not unique. If the building blocks are replaced by two original Goldberg 5*R* linkages, Wohlhart's double-Goldberg 6*R* linkage can be formed, in which the same bifurcation behaviour exists [32]. On the other hand, this double-Goldberg 6*R* linkage can be changed into a special case of the line-symmetric Bricard 6*R* linkage by using Wohlhart's isomerization method [33], as demonstrated in Fig. 20. The original link-pair 56–61 is replaced by a new link-pair 56′–6′1. The original and new link-pairs form a Bennett linkage. Thus, the geometry conditions of the special line-symmetric Bricard 6*R* linkage without offset are as follows.

$$
\begin{aligned}
&a_{12} = a_{45} = a - c,\ a_{23} = a_{56'} = d,\ a_{34} = a_{6'1} = b,\\
&\alpha_{12} = \alpha_{45} = \alpha - \gamma,\ \alpha_{23} = \alpha_{56'} = \delta,\ \alpha_{34} = \alpha_{6'1} = \beta,\\
&\frac{\sin\alpha}{a} = \frac{\sin\beta}{b} = \frac{\sin\gamma}{c} = \frac{\sin\delta}{d},\\
&R_i = 0(i = 1,\ 2, \dots,\ 6).
\end{aligned}
\tag{11}
$$

It should be expected that such a special Bricard linkage without offset also has four different forms, which can be transformed among each other through bifurcation points. The work on the general line-symmetric Bricard linkage will be addressed in an upcoming paper with more elaborations.

The double-subtractive-Goldberg 6*R* linkage presented in this paper belongs to the Bennett-based linkage in the viewpoint of construction. It is also closely related to the line-symmetric Bricard linkage in the viewpoint of bifurcation behaviour. Therefore, the linkage will play an important role in exploring the relationship between the Bennett-based linkages and the Bricard linkages. And the linkage's complicated bifurcation behaviour could be used for the design of reconfigurable mechanisms.

References

[1] G.T. Bennett, A new mechanism, Engineering 76 (1903) 777–778.
[2] G.T. Bennett, The skew isogram mechanism, Proceedings of the London Mathematical Society 13 (1914) 151–173.
[3] J.E. Baker, A comparative survey of the Bennett-based, 6-revolute kinematic loops, Mechanism and Machine Theory 28 (1993) 83–96.
[4] M. Goldberg, New five-bar and six-bar linkages in three dimensions, Transactions of the ASME 65 (1943) 649–663.
[5] F.E. Myard, Contribution à la géométrie des systèmes articulés, Bulletin de la Société Mathématique de France 59 (1931) 183–210.
[6] Y. Chen, Z. You, An extended Myard linkage and its derived 6R linkage, Transactions of the ASME: Journal of Mechanical Design 130 (5) (2008).
[7] K.J. Waldron, Hybrid overconstrained linkages, Journal of Mechanics 3 (1968) 73–78.
[8] H.C. Yu, J.E. Baker, On the generation of new linkages from Bennett loops, Mechanism and Machine Theory 16 (1981) 473–485.
[9] K. Wohlhart, Merging two general Goldberg 5R linkages to obtain a new 6R space mechanism, Mechanism and Machine Theory 26 (1991) 659–668.
[10] Y. Chen, Z. You, Spatial 6R linkages based on the combination of two Goldberg 5R linkages, Mechanism and Machine Theory 42 (2007) 1484–1498.
[11] C.Y. Song, Y. Chen, A spatial 6R linkage derived from subtractive Goldberg 5R linkages, Mechanism and Machine Theory 46 (2011) 1097–1106.
[12] C.Y. Song, Y. Chen, A family of mixed double-Goldberg 6R linkages, Proceedings of the Royal Society A 468 (2012) 871–890.
[13] R. Bricard, Mémoire sur la théorie de l'octaèdre articulé, Journal of Pure and Applied Mathematics 3 (1897) 113–150.
[14] R. Bricard, Leçons de cinématique, Gauthier-Villars, Paris, 1927.
[15] J.E. Baker, An analysis of the Bricard linkages, Mechanism and Machine Theory 15 (1980) 267–286.
[16] K. Wohlhart, A new 6R space mechanism, in: Congress on the Theory of Machines and Mechanisms, 1987, pp. 193–198.
[17] P.W. Fowler, S.D. Guest, A symmetry analysis of mechanisms in rotating rings of tetrahedra, Proceedings of the Royal Society A 461 (2005) 1829–1846.

[18] S.D. Guest, P.W. Fowler, A symmetry-extended mobility rule, Mechanism and Machine Theory 40 (2005) 1002–1014.
[19] Y. Chen, Z. You, T. Tarnai, Threefold-symmetric Bricard linkages for deployable structures, International Journal of Solids and Structures 42 (2005) 2287–2301.
[20] Y. Chen, W.H. Chai, Bifurcation of a special line and plane symmetric Bricard linkage, Mechanism and Machine Theory 46 (2011) 515–533.
[21] W.H. Chai, Y. Chen, The line-symmetric octahedral Bricard linkage and its structural closure, Mechanism and Machine Theory 45 (2010) 772–779.
[22] K. Wohlhart, Kinematotropic linkages, in: J.L.a.V. Parenti-Castelli (Ed.), The Fifth International Symposium on Advances in Robots Kinematics, Kulwer Academic Publishers, Portoroz, Slovenia, 1996, pp. 359–368.
[23] J.S. Dai, J.J. Rees, Mobility in metamorphic mechanisms of foldable/erectable kinds, Journal of Mechanical Design 121 (1999) 375–382.
[24] X. Kong, C. Huang, Type synthesis of single-DOF single-loop mechanisms with two operation modes, in: ASME/IFToMM International Conference on Reconfigurable Mechanisms and Robots, IEEE, 2009, pp. 136–141.
[25] K. Wohlhart, Multifunctional 7*R* Linkages, in: Proceedings of the International Symposium of Mechanism and Machine Science, AzCIFToMM, Izmir, Turkey, 2010, pp. 85–91.
[26] A. Müller, Generic mobility of rigid body mechanisms, Mechanism and Machine Theory 44 (2009) 1240–1255.
[27] A. Müller, Geometric characterization of the configuration space of rigid body mechanisms in regular and singular points, in: ASME 2005 International Design Engineering Technical Conferences & Computers and Information in Engineering Conference, Long Beach, California USA, 2005.
[28] W.W. Gan, S. Pellegrino, A numerical approach to the kinematic analysis of deployable structures forming a closed loop, Journal of Mechanical Engineering Science 220 (2006) 1045–1056.
[29] P. Kumar, S. Pellegrino, Computation of kinematic paths and bifurcation points, International Journal of Solids and Structures 37 (2000) 7003–7027.
[30] S. Pellegrino, Structural computations with the singular value decomposition of the equilibrium matrix, International Journal of Solids and Structures 30 (1993) 3025–3035.
[31] J. Denavit, R.S. Hartenberg, A kinematic notation for lower-pair mechanisms based on matrices, Transactions of the ASME: Journal of Applied Mechanics 22 (1955) 215–221.
[32] C.Y. Song, Y. Chen, The original double-Goldberg 6*R* linkage and its bifurcation analysis, in: International Symposium on Multibody Systems and Mechatronics (MUSME 2011), Valencia, Spain, 25–28 October, 2011.
[33] K. Wohlhart, On isomeric overconstrained space mechanisms on isomeric overconstrained space mechanisms, in: Congress on Theory of Machines and Mechanisms, 1991, pp. 153–158.